

Analytical Evaluation of High-Efficiency Induction Motor Losses

Aarniovuori Lassi, Lindh Pia, Kärkkäinen Hannu, Niemelä Markku, Pyrhönen Juha,
Cao Wenping

This is a Author's accepted manuscript (AAM) version of a publication

published by IEEE

in 2019 IEEE International Electric Machines & Drives Conference (IEMDC)

DOI: 10.1109/IEMDC.2019.8785380

Copyright of the original publication: © 2019 IEEE

Please cite the publication as follows:

Aarniovuori, L., Lindh, P., Kärkkäinen, H., Niemelä, M., Pyrhönen, J., Cao, W. (2019). Analytical Evaluation of High-Efficiency Induction Motor Losses. 2019 IEEE International Electric Machines & Drives Conference (IEMDC). DOI: 10.1109/IEMDC.2019.8785380

**This is a parallel published version of an original publication.
This version can differ from the original published article.**

Analytical Evaluation of High-Efficiency Induction Motor Losses

Lassi Aarniovuori

Power Electronics, Machines and
Power System Group
Aston University
Birmingham, UK
l.aarniovuori@aston.ac.uk

Markku Niemelä

Laboratory of Electric Drives
Technology
Lappeenranta University of Technology
Lappeenranta, Finland
markku.niemela@lut.fi

Pia Lindh

Laboratory of Electric Drives
Technology
Lappeenranta University of Technology
Lappeenranta, Finland
pia.lindh@lut.fi

Juha Pyrhönen

Laboratory of Electric Drives
Technology
Lappeenranta University of Technology
Lappeenranta, Finland
juha.pyrhonen@lut.fi

Hannu Kärkkäinen

Laboratory of Electric Drives
Technology
Lappeenranta University of Technology
Lappeenranta, Finland
hannu.s.karkkainen@lut.fi

Wenping Cao

Power Electronics, Machines and
Power System Group
Aston University
Birmingham, UK
w.p.cao@aston.ac.uk

Abstract— An analytical motor design-based approach is used to evaluate the major loss components of a premium-efficiency (IE3) four-pole squirrel-cage induction machine. In the analytical approach, the geometry of the machine and the material parameters are used to determine the loss components and they are compared with the ones obtained experimentally with IEC segregation of losses -method. The motor loss components under consideration are the stator copper, rotor copper, iron core, mechanical and additional load (residual) losses. The aim is to test the analytical calculation for further numerical optimization to improve the energy efficiency of the induction motors.

Keywords—Analytical calculation, efficiency, IEC, induction motor, iron losses, motor design, resistive losses.

I. INTRODUCTION

The efficiency of the electric motors is increasing, and more variable-speed motor drives are supplied instead of direct-on-line drives. Alternative motor technologies have been developed to improve the performance and energy efficiency of the electric machines. Synchronous reluctance and permanent magnet synchronous machines are becoming more popular in efficiency-critical variable speed applications. Some induction motors are designed to be used solely with a frequency converter supply and therefore the direct-on-line starting performance is no more a critical design parameter. Thus, the rotor resistance can be decreased. For converter-fed machines, a single cage structure instead of a double-cage is used.

Typically, a preliminary induction motor design is obtained using an analytical calculation process. This kind of processes are also used as a basis for different optimization algorithms. In optimization, different targets can be used, such as material price, torque quality or energy efficiency. Typically, the dimensioning equations are used to find the volume needed for the desired mechanical output power. The temperature rise allowed is one of the main dimensioning boundaries for electrical machines. In general, the higher the losses per volume in an electrical machine are, the higher is

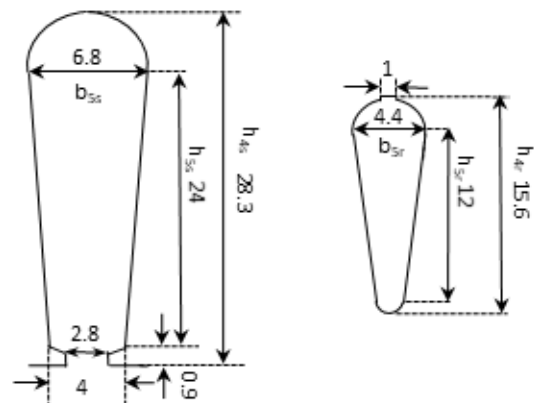


Fig. 1. The stator slot (left) and rotor slot (right) dimensions. The measures are given in millimeters (mm). The machine has stator slots, $Q_s=48$ and number of rotor slots is $Q_r=40$.

the temperature rise. The machine losses can be estimated using the design geometry and the material parameters. Nowadays, 2D finite element method (FEM) software is a basic tool to estimate the losses in electrical machines. Nevertheless, using 2D FEM to evaluate the induction motor losses has some problems. The 2D FEM software are using a circuit model that is used to couple the FEM solution to an external circuit and to model any 3D related effects. In the induction motors, the typical parameters that are inserted into the external circuit of the FEM model are the end winding resistance, the stator end-winding leakage inductance, and on the rotor side the short-circuit ring resistance and inductance. All these parameters have an effect on the loss results obtained with FEM. The stator winding resistance and rotor bar resistance for the parts that are inside the iron core are trivial to calculate if AC-induced losses are neglected and winding temperature is known, but the short-circuit ring parameters and the stator end winding are more complex to calculate. The iron losses are regularly calculated using Bertotti's model [1][2] and the users are adjusting empirical coefficients to match the losses based on priory knowledge about iron core material and measurements. Another problem is the slip: the static calculations are performed with fixed slip values and in the time-stepping calculations, the slip depends heavily on the

rotor losses and increased rotor resistance as the temperature rises.

The same input data that are needed to create the FEM model can be also used to construct a pure analytical model. The analytical model can be solved in a few seconds and the effect of the different parameters can be easily examined. This paper compares the analytically calculated loss components of an IE3-rated modern 5 kW single-cage induction motor with the losses obtained experimentally using the IEC segregation of losses method. The procedure followed here is part of the design process of an induction motor given in the book: Pyrhönen-Jokinen-Hrabovcova: Design of Rotating Electrical Machines [3]. It should be noted that there are some differences between the book editions 1 [3] and 2 [4]. In here, the aim is not to tweak any parameters, but to examine how close to measured values the analytical calculation procedure can reach in this case.

II. ANALYTICAL CALCULATION

The main dimensions and parameters of this squirrel-cage induction are given in the Table I.

A. Stator copper losses

For a three-phase induction motor, the stator copper losses (P_s) can be calculated using the stator AC resistance (R_{AC}) and the stator current (I_s) using the following equation

$$P_s = 3R_{AC}I_s^2. \quad (1)$$

However, the test subject here is a small motor with stator winding constructed with thin round enamelled copper wires and the DC-resistance can be used instead of AC-resistance. In addition, the difference between AC and DC copper losses is defined to be included in the additional losses in the IEC method that is used for loss comparison. The DC-resistance, denoted here as R_s of the machine is

$$R_s = \frac{Nl_{av}}{\sigma_{Cu}S_{Cu}}, \quad (2)$$

where N is the number of turns in series in the stator winding, l_{av} is the average length of a turn, σ_{Cu} is the specific conductivity of copper and S_{Cu} is the cross-sectional area of the conductor. Thus, to calculate the copper losses in the stator, we need the geometrical parameters for the stator slot and knowledge about winding configuration. The average length of a coil turn of a slot winding of a low voltage machine with round enamelled wires is approximately

$$l_{av} = 2l_w + 2.4 W_{ew} + 0.1 \text{ m}, \quad (3)$$

where l_w is the length of the conductor inside the stator core, W_{ew} is the coil span that is for full pitch windings

$$W_{ew} = \frac{\pi(D_s + h_s)}{2p}, \quad (4)$$

where D_s is the inner diameter of the stator, h_s is the stator slot height and p is the number of the pole pairs. The specific conductivity of the copper is adjusted to the design temperature using

$$\sigma_{Cu} = \frac{\sigma_{Cu,ref}}{1 + \alpha_{Cu}\theta_s}, \quad (5)$$

TABLE I
INDUCTION MOTOR PARAMETERS

Parameter	Value
Stator stack length	160 mm
Stator core outer diameter	220 mm
Stator core inner diameter	125 mm
Air gap	0.5 mm
Rotor core outer diameter	124 mm
Rotor core inner diameter	54 mm
Number of winding turns in one phase	128
Number of stator slots	48
Number of rotor slots	40
Winding configuration	Y
Rated voltage	400 V
Rated frequency	50 Hz
Rated power	5 kW
Number of pole pairs	2

where $\sigma_{Cu,ref}$ is the specific conductivity of the copper usually given at room temperature 20°C, α_{Cu} is the temperature coefficient of the resistivity of copper and θ_s is the designed temperature of the stator winding. Typical design temperatures for induction motors are 120°C and 145°C that correspond to 80 degrees temperature rise for insulation with class B temperature rise and 105 degrees for insulation with class 155 (F) temperature rise when the maximum ambient operating temperature is 40°C and 10°C hot spot margin is reserved. Here we use the measured temperature at the end of the heat run test that is $\theta_s = 102^\circ\text{C}$. The cross-sectional area S_c of the conductor in the stator slot can be calculated using basic geometry and dimensions given in Fig. 1. The cross sectional area of the single conductors is

$$S_c = \frac{k_{Cu,s}S_{Cu,s}}{az_{Qs}}, \quad (6)$$

where $k_{Cu,s}$ is the copper space factor in stator slot inside the slot insulation, $S_{Cu,s}$ is the total cross-sectional area of the stator slot, a is the number of parallel paths and z_{Qs} is the number of conductors in the slot. The cross sectional area of this simple slot geometry can be calculated by adding the area of the isosceles trapezoid and semicircle. The slot geometry dimensions must be reduced with the insulation layer thicknesses if that has not already been included in the space factor. The parameters used in the stator copper loss calculation are tabulated in the Table II.

B. Rotor copper losses

Similarly, as the stator copper losses, we can calculate the rotor copper losses (P_r) of a three-phase machine

$$P_r = 3R_r'(I_r')^2, \quad (7)$$

where R_r' is the rotor resistance and I_r' the rotor current of the single phase equivalent circuit referred to stator. The rotor bar resistance can be calculated with

$$R_{bar} = \frac{l_{bar}}{\sigma_{Al}S_{bar}}, \quad (8)$$

where l_{bar} is the rotor bar length, σ_{Al} is the specific conductivity of the aluminium and S_{bar} is the cross-sectional

TABLE II
STATOR LOSS CALCULATION PARAMETERS

Parameter	Variable	Value
Number of coil turns in series	N	128
Average length of a coil turn	l_{av} (m)	0.7095
Copper conductivity (@102°C)	σ_c (MS/s)	42.8
Cross sectional area of the stator slot	$S_{Cu,s}$ (mm ²)	148
Copper space factor	$k_{Cu,s}$	0.43
Stator resistance	R_s (Ω)	0.534
Stator copper losses	$P_{s,Cu}$ (W)	174

area of the rotor bar. Similarly, the end-ring portion of the resistance is

$$R_{ring} = \frac{l_{ring}}{\sigma_{Al} S_{ring}}, \quad (9)$$

where

$$l_{ring} = \frac{\pi D_{ring}}{Q_r}, \quad (10)$$

where D_{ring} is the average diameter of the end ring and Q_r is the number of rotor slots. The total rotor resistance is

$$R_r = R_{bar} + \frac{R_{ring}}{2 \sin\left(\frac{\pi p}{Q_r}\right)^2}, \quad (11)$$

where the argument of the sin function is the angular phase shift of the bar currents. When referring the rotor quantities to stator in electrical machines, the winding (k_{wv}) and skewing (k_{squ}) factors have to be taken into account and the referring factor is

$$\rho_v = \frac{4m_s}{Q_r} \left(\frac{Nk_{wv}}{k_{squ}} \right)^2, \quad (12)$$

where m_s is the number of stator phases. The values of the winding and skewing factors used here are given in Table II. Finally, the rotor resistance referred to stator is simply $R'_r = \rho_v R_r$. The parameters used in the rotor losses calculation are given in Table III.

C. Iron losses

The iron losses are slightly more complicated to calculate than the resistive losses. The iron losses can be calculated dividing the magnetic circuit into several sections where the flux density peak value is approximately constant and summing the losses of the different parts. The iron losses in a specific part can be estimated using

$$P_{Fe,n} = k_{Fe,n} P_{15} \left(\frac{\hat{B}_n}{1.5 \text{ T}} \right)^2 m_{Fe,n}, \quad (13)$$

where $k_{Fe,n}$ is an empirical correction coefficient to take into account the increase in the iron losses due to field harmonics and stresses created by punching. P_{15} is the material specific value of the losses of the material in Watts per kilogram with peak flux density of 1.5 T and frequency of 50 Hz. \hat{B}_n is the peak flux density of the part in question and $m_{Fe,n}$ is the mass of the part. The peak flux densities can be determined analytically in different parts of the machine using the peak flux density generated by the winding and the length of the iron circuit. The peak flux densities of the stator and rotor yokes are assumed equal. The iron cores of this motor have

TABLE III
ROTOR LOSS CALCULATION PARAMETERS

Parameter	Variable	Value
Bar resistance	R_{bar} (m Ω)	0.124
Rotor bar length	l_{bar} (mm)	160
Aluminum conductivity (@100°C)	σ_{Al} (MS/s)	26.9
Bar cross sectional area	S_{bar} (mm ²)	48
Length of SC-ring portion (mm)	(mm)	7.6
Cross sectional area of SC-ring (mm)	(mm ²)	375
Referring factor	ρ_v	4534
Rotor resistance referred to stator	R'_r (Ω)	0.63
Rotor copper losses	P_r (W)	121

TABLE IV
IRON LOSS CALCULATION PARAMETERS

Parameter	Variable	Value
Stator teeth correction coefficient	$k_{Fe,teeth}$	1.8
Stator yoke correction coefficient	$k_{Fe,yoke}$	1.6
Specific loss at (1.5 T, 50 Hz)	P_{15} (W/kg)	6.74
Iron losses	P_{Fe} (W)	228

TABLE V
MECHANICAL LOSS CALCULATION PARAMETERS

Parameter	Variable	Value
Bearing load	F (N)	128
Friction coefficient	μ	0.05
Inner diameter of the bearing	D_{bear} (mm)	42
Mechanical losses	P_{Fe} (W)	22

been constructed from electrical steel M800-65A and the material BH -curve is illustrated in Fig. 2. The coefficients used in the iron loss calculation are given in the Table IV. Naturally, the peak loss densities of the specific parts of the machine are needed to complete the calculation.

D. Mechanical losses

This motor does not have a fan mounted on the shaft. The motor has a low rotational speed and the windage losses originating from air movement can be neglected. Thus, the mechanical losses can be estimated using only the bearing friction losses

$$P_{friction} = 0.5 \Omega \mu F D_{bear}, \quad (14)$$

where Ω is the mechanical angular frequency of the motor, μ is the friction coefficient, F is the bearing load and D_{bear} is the inner diameter of the bearing that is the shaft diameter. The bearing load can be estimated using the mass of the rotor and dividing the force equally for drive- and non-drive end bearings. The parameters used in the mechanical loss determination are tabulated in Table V.

E. Additional load losses (Residual losses)

The additional load losses can be estimated based on an IEC-assigned value [5] that is for the rated powers of 1 kW to 1000 kW

$$P_{LL} = P_1 \left[0.025 - 0.005 \log_{10} \left(\frac{P_2}{1 \text{ kW}} \right) \right], \quad (15)$$

where P_1 is the input power and P_2 the shaft power. Eq. (15) gives 2.46% of the input power for a 5 kW machine. However, it is known that the measured additional load losses are far below the IEC allowance and here we use 1.2% of the input power that is the average value for 5 kW machines found from the collated test results presented in [6]. Overestimation of the

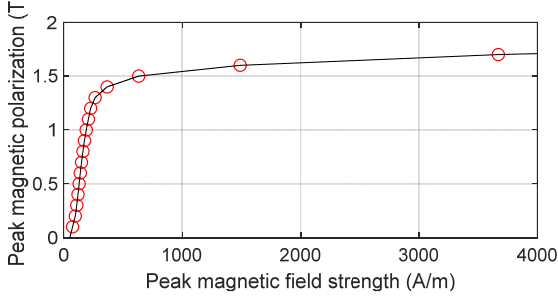


Fig. 2. BH -curve of the M800-65A. The material is used in the construction of the test machine's iron cores. The red dots show the table values and the black continuous line the fitted curve used.

additional load losses is not always a bad thing and it gives some safety margin for manufacturing tolerances.

III. SEGREGATION OF LOSSES

The segregation of losses is an indirect efficiency determination method where the losses of the machine are determined performing three tests: rated load heat-run test, load curve test and no-load test [7]. The procedure followed here is based on IEC but the IEEE counterpart 112B does not have significant differences [8]. The indirect method is beneficial especially for high efficiency machines, since the loss uncertainty is approaching infinity when the machine efficiency is approaching unity when using the efficiency determination method based on the input and output powers. The new motor was driven to its thermal equilibrium several times before conducting the actual tests to allow the relaxation of some manufacturing stresses in the iron parts and to get the bearing lubrication to a normal level. The nameplate values of the new design are not available because this is a special machine for research purposes. Therefore, the rated load heat run test is used to obtain the rated values of current, slip and power factor. The measured rated current value was 10.4 A RMS and the no-load stator current values was 6.1 A RMS.

A. Stator copper losses

In IEC procedure, the stator copper losses P_s are calculated multiplying the test resistance R measured from motor terminals and the square of the stator current RMS value during the heat run test

$$P_s = 1.5 R I^2. \quad (16)$$

The test resistance (R) is corrected to the actual winding temperature at the end of the heat run test using

$$R_{\theta_w} = R_{\theta_{amb}} [1 + \alpha_{Cu}(\theta_w - \theta_{amb})], \quad (17)$$

where $R_{\theta_{amb}}$ is the ambient temperature, that is equal the winding temperature of the cold machine during the resistance measurement, θ_w is the winding temperature at the end of heat run test, and α_{Cu} is the temperature coefficient for the resistance of copper. In here, a four-wire resistance measurement was used to measure the cold machine stator resistance and the temperature of the windings was measured using pre-installed Pt-100 sensors to adjust the test resistance. Finally, the copper losses were adjusted to reference temperature

$$P_{s,\theta} = k_\theta P_s, \quad (18)$$

where k_θ is the temperature correction factor, that is calculated using the winding temperature (θ_w) and θ_{amb} ambient temperature for copper windings as follows

$$k_\theta = \frac{235 + \theta_w + 25 - \theta_{amb}}{235 + \theta_w}. \quad (19)$$

B. Rotor copper losses

The rotor copper losses are calculated using the electric input power during the heat run test (P_1), the corrected stator copper losses, iron losses (P_{Fe}) and the slip value (s) at the end of the heat run test

$$P_{r,\theta} = (P_1 - P_{s,\theta} - P_{Fe})k_\theta s. \quad (20)$$

C. Iron losses and mechanical losses

The iron and mechanical losses are determined from constant losses

$$P_k = P_0 - 1.5 R_{s,0} I_{s,0}^2 = P_{Fe,0} + P_{mech,0}, \quad (21)$$

where P_0 is the electric input power during the no-load test, $R_{s,0}$ is the linearly interpolated resistance from the measured values with the no-load input power, $I_{s,0}$ is the measured no-load current and $P_{Fe,0}$ is the no-load iron loss. To calculate the mechanical losses, constant losses are plotted as a function of the square of the fundamental voltage as illustrated in Fig. 3. The no-load mechanical losses $P_{mech,0}$ are linearly extrapolated from the four lowest constant loss points at zero voltage. Since the mechanical losses depend on the rotational speed of the motor, the no-load mechanical losses are corrected to rotational speed at the end of the heat run test using

$$P_{mech} = P_{mech,0}(1 - s)^{2.5}. \quad (22)$$

The four highest constant loss points are used for interpolating the rated load iron losses. The iron loss curve is the difference between the constant loss curve and the no-load mechanical losses. The rated load iron loss P_{Fe} is found from the interpolated iron loss curve at the inner voltage U_i , which takes the stator winding voltage drop into account

$$U_i = \sqrt{\left(U - \frac{\sqrt{3}}{2} I R \cos \varphi\right)^2 + \left(\frac{\sqrt{3}}{2} I R \sqrt{1 - \cos^2 \varphi}\right)^2}, \quad (23)$$

where the voltage, current and phase angle (φ) values are from the heat run test. The iron loss determination based on IEC 60034-2-1 is presented in Fig. 4.

D. Additional load losses (Residual losses)

According to IEC, the additional load losses are the residual losses at the rated operating point

$$P_{Lr} = P_1 - P_2 - P_s - P_r - P_{Fe} - P_{mech}, \quad (24)$$

where the stator and rotor copper and the mechanical losses are the uncorrected losses while the iron losses are the rated operating point losses. In the load curve test, the motor load

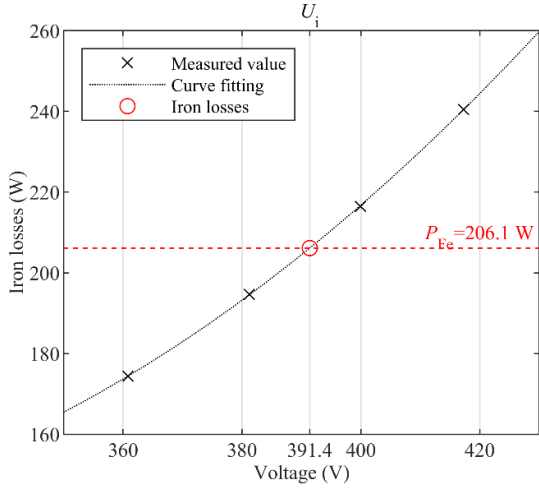


Fig. 3. Iron losses determination from no-load data points according to IEC 60034-2-1.

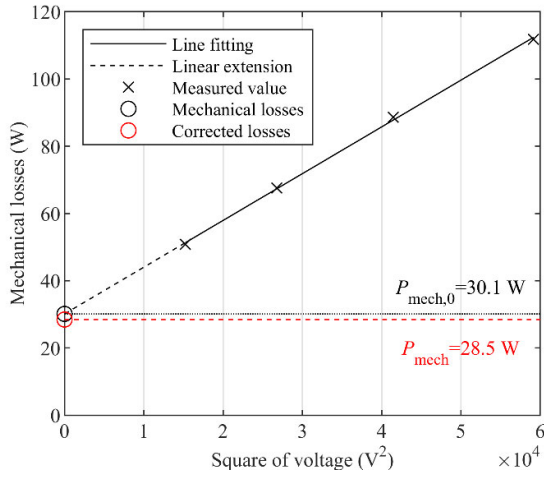


Fig. 4. Mechanical losses determination from experimental no-load test data points according to IEC 60034-2-1.

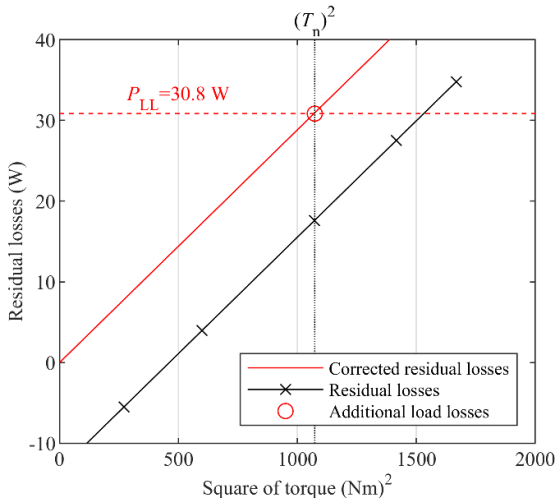


Fig. 5. Additional load losses determination from load curve data points according to IEC 60034-2-1.

is rapidly varied, and it is assumed that the temperature of the machine and all the fundamental loss components remain relatively constant during the test and the difference between the losses calculated using the electrical input power and

shaft power and the individual loss components are the additional load losses. The additional load loss determination from residual losses is illustrated in Fig. 5. The residual losses are plotted as the function of the square of the torque and a line fitting for the residual loss points is performed. Finally, the line-fit is moved to pass through origin and the additional loss value is found at nominal torque squared.

IV. LOSS COMPARISON

To calculate the losses analytically the stator and rotor currents have to be determined, which is conducted with the help of the single-phase steady-state equivalent circuit. The additional load losses portion can be added to iron losses when determining the iron loss resistance for machine operating point determination

$$R_{Fe} = \frac{3(U_i)^2}{P_{Fe} + P_{LL}}, \quad (25)$$

The loss components comparison is not valid if the stator current values are not comparable. While performing the initial calculations, it was noted that the magnetizing current value was not exactly correct and therefore the comparison of the resistive losses could not be performed meaningfully.

A. Magnetizing inductance

Magnetizing inductance is an extremely important parameter in defining the induction motor loss distribution, since the magnetizing energy is fed through the stator and it sets the value of the magnetizing current. The magnetizing inductance can be calculated using the no-load test data

$$L_{m,meas} = \frac{U_0}{2\pi f_s I_m}, \quad (26)$$

where U_0 is the measured no-load voltage, f_s is the supply frequency and I_m the magnetizing current

$$I_m = I_{s,0} \sin \varphi_0, \quad (27)$$

where φ_0 is the measured phase angle. On the other hand, it can be calculated using

$$L_m = \alpha_i \mu_0 \frac{m_s \tau_p}{2} \frac{4 l'}{2p \pi \delta_{eff}} (Nk_{w1})^2, \quad (28)$$

where α_i is a saturation factor, μ_0 vacuum permeability, τ_p is the stator pole pitch, l' is the equivalent core length of the machine and δ_{eff} is the length of the effective air-gap and k_{w1} is the winding factor for fundamental component. In this machine, the iron parts do not saturate substantially at the rated operation point and we can use $\alpha_i = 2/\pi$ value that corresponds to sinusoidal flux density distribution across a pole pitch. In most designs, especially in case of DOL supply, it is recommendable to let the tooth tips to saturate and then the saturation factor must be iterated to its correct value. The measured magnetizing inductance is 123 mH and the magnetizing current 6.0 A RMS while the initially calculated value is 136 mH. The magnetizing inductance is directly proportional to the effective length l' of the core and inversely proportional to the effective air-gap length δ_{eff} that is

$$L_m \propto \frac{l'}{\delta_{\text{eff}}}. \quad (29)$$

Since $l' \gg \delta_{\text{eff}}$ and we know that punching and machining reduce the permeability of iron on the boundaries of the iron sheets [9] making the air-gap behave as a lengthier one and making slot openings magnetically wider further increasing the effective air gap when the Carter factor is calculated. It is, therefore, justified to adjust the air-gap length. This has been traditionally taken into account by an empirical factor, and the air-gap length is increased by 0.1 mm on both sides. However, a 0.7 mm air-gap value leads to 6.7 A RMS magnetizing current in this machine that is already too high. The correct magnetizing inductance value can be found when the physical air-gap is increased from 0.5 mm to 0.57 mm. The motor parameters are compared in Table VI with the measured values after the air-gap is adjusted. The loss comparison is illustrated in Fig. 6. In principle, the analytically calculated loss components are close to measured ones. The analytically calculated total losses of the machine are 610.7 W while the measured total losses are 570.4 W and the difference is only 7% of the total losses that can be considered a good result.

V. DISCUSSION

The stator resistance and the resulting stator copper losses are smaller than the measured values. There are several possible reasons for that: In here, the pure copper conductivity is used, but if there are impurities in copper, the resistivity is increased. The length of the stator end winding has a major role in the stator resistance determination since the stator core length is 160 mm and the average length of the single end winding is estimated to be 190 mm. In here, we can easily have a significant mistake, since estimating the end-winding length to be 220 mm, the resulting winding turn length would be extended by 10% that is also in direct relation to the stator resistance, Eq. (2). The most problematic part in the induction machine loss analysis with analytical means is the additional load losses. Part of the additional load losses are formed by the saturation of the tooth tips and associated with increase in harmonics that are complicated to model analytically but are relatively easy to study with finite element methods. In small

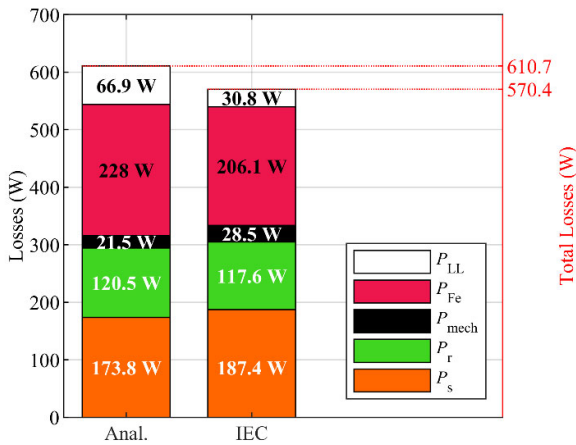


Fig. 6. The loss components obtained analytically and the measured values using IEC-segregation of losses

TABLE VI
MEASURED AND CALCULATED PARAMETERS

Parameter	Measured	Analytical
Stator current, I_s (A)	10.4	10.3
Phase resistance $R_{s, \text{phase}}$ (Ω)	0.582	0.534
Magnetizing inductance L_m (H)	0.123	0.123
Rated speed n_n (rpm)	1467	1465
Slip, s_n	2.2	2.3
Power factor, $\cos \varphi$	0.78	0.79
Efficiency, η (%)	89.0%	89.2%

machines the additional load losses form a relatively minor part of the total losses, but in larger machines they become more significant [9] especially because of the AC-resistance increase as a result of skin effect.

Since the additional load losses are relatively small part of the losses, they do not affect the accuracy of the other loss components calculation due to incorrect current drawn by the machine.

Analytical tools are still a valuable way to examine the overall design and material choices and to get a preliminary design to be studied in depth with other methods. The resistive losses can be matched by adjusting the conductivities of the stator and rotor winding materials without significant effect on other parameters.

VI. CONCLUSION

The analytical calculation process without any parameter modifications shows mediocre accuracy performance. The magnetizing inductance or current must be adjusted to calculate the loss components of the machine with reasonable accuracy. The measured iron losses correspond well with the ones calculated analytically. The same uncertainty related to design parameters that are used in the loss calculation of electrical machines exists for both analytical methods and FEM. Without a prior knowledge and without matching any of the calculation parameters with the measured values of the prototype machines, it is a coincidence to get identical values with calculation methods and measurements.

REFERENCES

- [1] G. Bertotti, "Physical interpretation of eddy current losses in ferromagnetic materials. I. Theoretical considerations, *Journal of Applied Physics*, vol. 57, no. 6, pp. 2110-2117, Mar. 1985.
- [2] G. Bertotti, "Physical interpretation of eddy current losses in ferromagnetic materials. II. Analysis of experimental results, *Journal of Applied Physics*, vol. 57, no. 6, pp. 2118-2126, Mar. 1985.
- [3] J. Pyrhönen, T. Jokinen and V. Hrabovcova, "Design of Rotating Electrical Machines," 2nd Ed., John Wiley & Sons, Ltd, 2014
- [4] J. Pyrhönen, T. Jokinen and V. Hrabovcova, "Design of Rotating Electrical Machines," 1st Ed., John Wiley & Sons, Ltd, 2008.
- [5] IEC, "Rotating electrical machines – Part 2-1: Standard methods for determining losses and efficiency from tests (excluding machines for traction vehicles)", Ed. 2, IEC 60034-2-1, June 2014.
- [6] E. B. Agamloh, "An Evaluation of Induction Machine Stray Load Loss From Collated Test Results," in *IEEE Transactions on Industry Applications*, vol. 46, no. 6, pp. 2311-2318, Nov.-Dec. 2010.
- [7] H. Karkkainen, L. Aarniovuori, M. Niemela and J. Pyrhonen, "Converter-Fed Induction Motor Efficiency: Practical Applicability of IEC Methods," in *IEEE Industrial Electronics Magazine*, vol. 11, no. 2, pp. 45-57, June 2017.
- [8] A. Boglietti, A. Cavagnino, M. Lazzeri, and M. Pastorelli, "Induction motor efficiency measurements in accordance to IEEE 112-B, IEC 34-2 and IEC 37 international standards," in *Proc. IEEE Int. Electric*

Machines and Drives Conference 2003, vol. 3, Madison, USA, June 2003, pp. 1599–1605.

- [9] A. Saleem, “Effect of Manufacturing on Microstructure and Magnetic Properties of Non-Oriented Electrical Steel”, Doctoral thesis, McGill University, Montreal, Nov. 2017.

- [10] L. Aarniovuori, M. Niemelä, J. Pyrhönen, W. Cao and E. B. Agamloh, “Loss Components and Performance of Modern Induction Motors,” *2018 XIII International Conference on Electrical Machines (ICEM)*, Alexandroupoli, 2018, pp. 1253-1259.